Impacts of Climate Change on River Flows in the Upper Indus Basin and Its Subbasins

Sohaib Baig (aquarius_baig@yahoo.com)
Kyoto University: Kyoto Daigaku
Takahiro Sayama
Kyoto University: Kyoto Daigaku
Masafumi Yamada
Kyoto University: Kyoto Daigaku

Research article

Keywords: Upper Indus Basin, Climate Change, River Flows, Hydrology, Pakistan

Posted Date: April 20th, 2021

DOI: https://doi.org/10.21203/rs.3.rs-404691/v1

IMPACTS OF CLIMATE CHANGE ON RIVER FLOWS IN THE UPPER INDUS BASIN AND ITS SUBBASINS

Sohaib Baig[1]

Corresponding author

Email: baig.sohaib.2s@kyoto-u.ac.jp and aquarius_baig@yahoo.com

Takahiro Sayama[1]

Email: sayama.takahiro.3u@kyoto-u.ac.jp

Masafumi Yamada[1]

Email: yamada.m.hydra@gmail.com

(Institutional addresses)

[1] Disaster Prevention Research Institute, Kyoto University, Uji, Japan

Abstract

The upper Indus river basin (UIB) has a cold climate and generates vital runoff annually. This runoff is very important for sustainable water supply and agriculture in the region. Runoff in

UIB consists of rainfall, snow and glacier melt. Winter precipitation in the basin is essential for the replenishment of glaciers which is the most dominant runoff source. Climate change may alter the runoff generation in the basin and affect the availability of water for consumption. This study employs a hydrologic model and a fine resolution MRI-AGCM (0.1875°) to quantify the impacts of climate change on river flows in UIB and its sub-basins. The simulations of river flows have shown satisfactory results when compared with observed ones. Furthermore, simulated snow-cover is compared with estimated snow-cover by MODIS and has shown good agreement. According to simulation results glaciers alone contribute two-third in the annual river flows at UIB while rainfall and snow contributes 19 and 11% respectively. Future (2075-2099) temperature will increase in every season across the UIB, highest increase is projected to take place in September-October with approximately 8 °C. While, on annual basis the temperature will increase by 5 °C. Likewise, precipitation will increase every month across UIB, specifically the increase in July-August period is very significant. Albeit the precipitation increase is highly variable on spatial scale i.e. decreasing/increasing at same time in different regions. This variable behavior of future precipitation will result in verities of hydrographs in UIB and its sub-basins. Overall in UIB the annual river flows will decrease by 16% with significant seasonal variations. Summer flows will decrease and spring flows will increase because of glacier retreat and higher precipitation. Sub-basins' response is mixed with

increasing and decreasing because of different topography, climate and other factors. These changes necessitate a more holistic approach in mitigating the changes in the water availability.

Keywords

Upper Indus Basin, Climate Change, River Flows, Hydrology, Pakistan

Introduction

The Indus River basin covers an area of 1,140,000 km^2 in Afghanistan, China, India, and Pakistan. The length of the river is approximately 2,800 km, and its origin lies in Tibet (Figure 1) (Ali, 2013). In the northern parts (Figure 1), the basin receives runoff from the Himalaya, Karakoram, and Hindukush mountains, which mostly consists of melt from snow and glaciers (Lutz et al., 2014). This upper Indus basin (UIB) supplies flows of surface water essential to one of the world's largest contiguous canal irrigation systems (Lutz et al., 2016).

Climate in the UIB is very variable, with sub-freezing winter temperatures, while the average temperatures in summer (May to September) is approximately 15 °C. Winter persists from October to March and temperatures remain below 0 °C (Mcsweeney et al. 2012). Precipitation also shows significant spatial and temporal variabilities, and the unavailability of dense networks of climate stations makes the available data unreliable. Several studies have employed techniques to quantify accurate precipitation in the UIB. For example, Reggiani and Rientjes

56 (2015) used the mass-balance technique and estimated the total annual precipitation in the basin
57 to be 681 ± 100 mm. Similar estimates of total annual precipitation have been reported by Dahri
58 et al. (2018) and Immerzeel et al. (2015). In winter, precipitation falls as snow accumulates in
59 the season and melts in spring; this meltwater from snow and glaciers results in higher flows
60 from July to September (Mukhopadhyay and Khan, 2014).
61 Runoff in the UIB consists of rainfall, snow, and glacier melt, and peak flows occur in summer
62 when snow and glaciers melt (Archer 2003). At the downstream of Bisham Qila, the Tarbela
63 Reservoir supplies water essential for irrigation, stores flood water, and generates hydropower
64 (Figure 1) (Lutz et al. 2016).
65 Because of climate change, the hydrological cycle is under stress. Rising temperatures will
66 cause more water to evaporate, which will increase the moisture content in the atmosphere and
67 render the spatiotemporal trends in precipitation more variable (Wester et al. 2019). In addition
68 to precipitation variability, the increased temperature will alter the hydrological cycle in the
69 UIB because runoff largely depends on melt from snow and glaciers (Immerzeel et al., 2010).
70 Understanding future climate is necessary for water management in the region and meeting
71 downstream demands. Future climate change in the Himalayan–Karakoram region, where the
72 UIB is located, has been projected by Sanjay et al. (2017) using dynamic downscaling of
73 regional climate models (RCMs). According to these projections, temperatures will increase

74 between 2 °C to 3.1 °C under the RCP 4.5 scenario; according to the RCP 8.5 scenario, the
75 temperature increase will be in the range of 2.7 °C to 5.4 °C. Similarly, an increase in
76 precipitation of up to 14% is projected across RCP 4.5 and 8.5.
77 Glaciers in the region will not be able to retain their mass despite the increase in precipitation
78 because the increase in temperatures will make the current mass balance negative. This situation
79 will result in an increase in glacier melt rates in the coming decades until the last quarter of this
80 century (Rounce et al. 2020).
81 From the perspectives of water resources management and water-related hazard risk
82 management, projections of the spatial distributions of river flows within the UIB and the whole
83 river basin are crucial. Therefore, this study focuses on the entire UIB as well as three
84 representative subbasins to reveal their responses to climate change. The three selected
85 subbasins have different topography and climate characteristics, which are ideal for
86 understanding inter-basin variability. This study employs a fine-resolution Meteorological
87 Research Institute atmospheric general circulation model (MRI-AGCM) with a spatial
88 resolution of 0.1875°. The model simulates four scenarios based on different spatial patterns in
89 sea surface temperatures. The objectives of this study are as follows:
90 a) Simulate the hydrological cycle of the UIB with a distributed hydrological model forced by
91 observed climate datasets. Snow and glacier melt models are coupled with the hydrological

92 model based on geographic datasets including land use and glacier cover datasets. By
93 conducting various scenario simulations, we quantify the runoff components of river flows from
94 different sources including rainfall, snowmelt, and glacier melt.
95 b) Quantify the impacts of climate change on the stream flow of the UIB and its subbasins. The
96 runoff components are projected under future climate conditions to better understand future
97 stream flow changes in the entire UIB and its subbasins.
98

99 **Study Area and Used Data**

100 The distribution of elevation and other details of the UIB and subbasins are shown in Figure 2
101 and Table 1. The basin has a maximum elevation of 7,528 m. The total area of the basin is
102 192,861 km^2. About two-thirds of the total area lies between the elevations of 3,500 and 5,500
103 m. In general, the eastern subbasins have higher altitudes than the western subbasins.
104 The glacier cover was extracted from a dataset prepared by the International Centre for
105 Integrated Mountain Development (ICIMOD), which contains detailed information related to
106 clean and debris-covered glaciers (ICIMOD, 2011). Figure S1 a and Figure S1 b show the
107 spatial distribution of glaciers in the basin. The total glacier area in the basin is 7,912 km^2, and
108 most of the mass is concentrated in the northwestern region. Shigar has the largest glacier
109 covered area with 28% glacier cover, followed by Gilgit and Kharmong (Table 1). In Shigar

and Gilgit glacier melt forms the largest proportion of annual runoff (Mukhopadhyay and Khan, 2015).

The observed monthly discharge (1980–2005) at Bisham Qila is shown in Figure S2. Even in winter (October–April) with limited rainfall, the average monthly flow is sustained at approximately 450 m^3/s. This base flow is mainly due to the snow and glacier melt, as explained by Mukhopadhyay and Khan (2015). The flow regime between May and September is important because of its considerable contribution to meeting the water demands of the entire Indus River basin.

Figure S3 shows the frequency distribution of the daily river flow at Bisham Qila. The daily discharge corresponding to the non-exceedance probability or 99% (Q99) was 12,452 m^3/s, and Q75, Q50, and Q25 are 10,380 m^3/s, 6,915 m^3/s, and 3,463 m^3/s, respectively.

For hydrological modeling of river flows, the Asian precipitation highly resolved observational data integration towards evaluation (APHRODITE) (Yatagai et al. 2012) climate dataset was used along with glacier cover (ICIMOD 2011). Figure 3 and Figure S4 show seasonal precipitation and temperature variation in the basin. The original APHRODITE dataset of precipitation was corrected using the precipitation extrapolation rate and topographic controls (Immerzeel et al., 2015). According to the dataset, winter (November to April) receives more precipitation than summer (May to October). Higher elevation zones receive heavy

precipitation in winter in the form of snowfall. The eastern edge of the UIB is shown to have a high rate of precipitation in summer because it coincides with the western Himalayas, where the monsoon season is dominant. On an annual basis, the southern edges and eastern region of the UIB receive higher precipitation. Winter receives heavy snowfall due to western disturbances, and the monsoon climate causes precipitation in July and August.

The temperatures are lower in the northern and eastern regions of the UIB, while the lower elevation zones in the west are warmer (Figure 3). The annual average temperature is between 12 and −8 °C (Figure 3).

Method

The grid-based model based on the rainfall–runoff–inundation (RRI) model introduced below was run with snow and glacier melt models. The rainfall, snowmelt, and glacier melt were calculated for each grid and used to simulate river flows. For snow and glacier melt, degree-day melt models were used. These models require daily precipitation, daily temperature, and topographic information (Figure 4).

The simulation period consisted of twenty-six years from 1980 to 2005. The simulation was divided into two periods, one for calibration and other for validation. The calibration covered 13 years from 1980 to 1992, while validation covered 13 years from 1993 to 2005. The model

146 was calibrated and validated with observed river flows at Bisham Qila, and the performance
147 was checked using several statistical parameters. River flows at subbasins were validated with
148 observed river flows and simulated snow covers were compared with Moderate Resolution
149 Imaging Spectroradiometer (MODIS) snow cover.
150

151 **Cema-Neige snow melt model**

152 The Cema-Neige snow melt model was adopted from Valéry et al. (2014). This is a degree-day
153 melt model that uses maximum T_{max}, minimum (T_{min}), and mean air temperatures (T_{mean}) to
154 distinguish between rainfall and snowfall. It has an additional feature of calculating the
155 percentage of snow (P_s) in precipitation.
156 If the maximum temperature is below 0 °C, all precipitation is considered snow, i.e., 100%. If
157 the minimum temperature is above 0 °C, all precipitation is rainfall. In all other cases, the
158 percentage is estimated by employing the third expression in Eq. (1).

159 $$P_s = \begin{cases} 1 & if\ T_{max} < 0\ ^\circ C \\ 0 & if\ T_{min} > 0\ ^\circ C \\ 1 - \dfrac{T_{max}}{T_{max} - T_{min}} \end{cases} \quad (1)$$

160 The quantities of rainfall and snowfall are calculated using Eqs. (2) and (3):

161 $$P_{snow} = P_s * P \quad (2)$$

162 $$P_{rain} = P - P_{snow} \quad (3)$$

where P_{snow} is the snow precipitation (mm/d), P is the precipitation (mm/d), and P_{rain} is the liquid precipitation (mm/d). The snowpack temperature ($Snowpack_{temp,t}$) defines the internal thermal state of the snowpack, which is used to quantify the melt. If the internal temperature rises to 0 °C, the melt takes place. Eq. (4) estimates the snowpack temperature.

$$Snowpack_{temp,t} = \min \begin{cases} 0 \\ X * Snowpack_{temp\,t-1} + (1 - X) * T_{mean} \end{cases} \quad (4)$$

where $Snowpack_{temp,t}$ is the snowpack temperature, °C, and X is the snowpack inertia factor, which is set by calibration. The potential melt, $Melt_{pot}$ (mm/d), is computed when the snowpack temperature reaches 0 °C and the mean air temperature is greater than 0 °C.

$$Melt_{pot} = ddf * T_{mean} \quad (5)$$

where ddf is the degree-day factor. The melt cannot exceed snow storage. In such a case, $Melt_{pot}$ is restricted to snow storage. Accumulation of snowfall is an important part of the Cema-Neige model. The accumulation is updated daily based on the previously stored snow and the sum of P_{snow} of a particular day as indicated by Eq. (6).

$$SS_{update} = SS_{update,t-i} + P_{snow,t} - Melt_{act} \quad (6)$$

where SS_{update} (mm) is the snow storage update after accumulation and melt of snow, SS is the snow storage (mm), and $Melt_{act}$ is the actual melt (mm/day). Actual Melt, $Melt_{act}$ (mm/d), is estimated by an empirical expression (Eq. (7)). The snow cover area is also employed in this function:

$$Melt_{act} = (0.9 * snow\ cover\ area + 0.1) * Melt_{pot} \quad (7)$$

Snow cover area (%) is a unique and simple feature of the model. The model uses P_{snow} and annual average snowfall to estimate the percentage of the river basin covered with snow (Eq. (8)).

$$snow\ cover\ area = \begin{cases} SS_t/TPS & if \quad SS_t < 0.9 * Z \\ 1 \end{cases} \quad (8)$$

where Z is the average annual snow precipitation (mm). More detailed information on Cema-Neige can be found in Valéry et al. (2014).

Glacier melt model

The glacier cover of the region estimated by ICIMOD (2011) was used to calculate the melt from each grid. The glacier melt was quantified using a degree-day model explained by Terink et al. (2015). Eq. (9) was used to calculate the daily melt from clean ice and debris-covered glaciers.

$$A_{CI} = \begin{cases} T_{avg} \ . DDF_{CI} \ . F_{CI} & if \quad T_{avg} > 0 \\ 0 & if \quad T_{avg} \leq 0 \end{cases} \quad (9)$$

In the above equation, $A_{CI/DC}$ refers to daily glacier melt from clean ice and debris-covered glaciers, $DDF_{CI/DC}$ (mm C^{-1} day^{-1}) are degree day factors, and $F_{CI/DC}$ are the proportion of clean ice and debris-covered glaciers in the grid. The degree-day factors are set by calibration. The total glacier melt is the sum of both $A_{CI/DC}$ (Eq. (10).

$$A_{GLAC} = (A_{CI} + A_{DC}) \quad (10)$$

199

200 **GCM Downscaling**

201 MRI-AGCM is a general circulation model (GCM) with a spatial resolution of 20 km. The
202 present climate is simulated using observed sea-level temperatures and it shows satisfactory
203 performance in the global distribution of tropical cyclones, the East Asian monsoon, etc.
204 (Mizuta et al. 2012).

205 The delta-change method was selected to remove the biases in temperature present in the MRI-AGCM.
206 This method is a widely used technique that considers the mean bias as the difference between the
207 observed and GCM data (Miao et al. 2016). The future data are adjusted using this bias. The future
208 projection can be adjusted as:

209 $$\tilde{x}_{m-p.adjust} = x_{m-p} + (\bar{x}_{o-c} - \bar{x}_{m-c}) \qquad (11)$$

210 where x is the meteorological variable of either o (observed) or m (modeled) for a historic training
211 period or current climate (c) or future projection (p). Linear correction is another bias-correction
212 technique that utilizes a scaling factor between observed and GCM simulations to reduce the bias in
213 future projection. This is used for the bias correction of precipitation data as suggested by many previous
214 studies (for example, Miao et al., 2016).

215 $$\tilde{x}_{m-p.adjust} = x_{m-p} \cdot \left(\frac{\bar{x}_{o-c}}{\bar{x}_{m-c}}\right) \qquad (12)$$

Future climate scenarios in the UIB and subbasins are explained with the help of figures in the results section.

RRI Model

The runoff generated from the Cema-Neige model for snowmelt and the glacier melt model described above was used as an input for the RRI model. The RRI model is a two-dimensional model that is capable of simultaneously representing rainfall runoff and flood inundation (Sayama et al. 2012). The flow on the slope grid cells was calculated using the 2D diffusive wave model, while the channel flow was calculated using the 1D diffusive wave model. For better representations of rainfall–runoff–inundation processes, the model simulates lateral subsurface flow, vertical infiltration flow, and surface flow. The vertical infiltration flow was estimated using the Green–Ampt model (Sayama 2015).

Glacier Area

In this study, the future glacier area was extracted from the estimates given by Huss and Hock (2015). This study simulated the average glacier area in the future using 14 GCMs for the western parts of South Asia, where the UIB is located. Projected average glacier area for the entire western South Asia by 2075-2099 is 9,144 km^2. This is roughly 28% of the present area,

234 which is 32,814 km^2 (Figure S5). In this study, we assume the same ratio of glacier loss in the
235 UIB region as estimated by Huss and Hock (2015) for the entire region of western South Asia.
236 Thus, we assume that the current glacier area of 7,912 km^2 in the UIB (ICIMOD, 2011) will
237 reduce to 2,215 km^2 by 2075-2099. In terms of the spatial variation of the glacier cover under
238 future climate conditions, we also theorize that the glacier area will mainly be lost from the
239 lowest elevation areas due to the higher temperatures.
240

241 Results and Discussions

242 Model Calibrations and Validations

243 The simulated discharge at Bisham Qila is shown in Figure 5, and the model performance is
244 summarized in Table 2. Both the simulated and observed hydrographs show good agreement,
245 however with some inconsistencies.
246 A comparison of snow-covered areas obtained from the Cema-Neige model and MODIS is
247 shown in Figure 6, which shows snow cover from 2000 to 2005. The model does not consider
248 the slope and aspect of the grid cell in the simulation, so it is not the exact representation of the
249 physical process. In addition, an important parameter of the Cema-Neige model is the division
250 of precipitation into rainfall and snowfall, which is based on using a 0 °C threshold. These
251 factors are the sources of disagreement between the model results and the actual snow cover.

252 Overall, simulations show satisfactory results, but improvements are required in the calibration
253 of summer flows. The comparison of runoff components with other studies suggests agreements
254 on the quantity.
255
256 **Estimation of Snow and Glacier Contributions Under Present Climate**
257 Figure 7 shows the monthly contribution of rainfall, snowmelt, and glacier melt. Under the
258 current climate conditions, glaciers contribute 68%, rainfall 20%, and snowfall 12% of river
259 flows. Rainfall runoff is generated in the monsoon months (August and September), and the
260 annual maximum rainfall discharge (September) is approximately 650 m^3/s. With the increasing
261 temperature in April, snow starts to melt from the lower elevation zones, and its discharge
262 reaches approximately 1000 m^3/s in April and approximately 2400 m^3/s in May. The initiation
263 of high flows in the hydrograph is due to the snowmelt in April (80%) and May (73%).
264 Meltwater from higher zones, specifically glacier-melt, follows snowmelt. In summer from
265 June to September, glaciers contribute 85% of the total flow. In August, glacier flow reaches a
266 maximum with an average discharge of approximately 5600 m^3/s. The glacier melt estimate
267 was compared with that of other studies (e.g., Lutz et al. 2014; Mukhopadhyay and Khan, 2015;
268 Hassan et al. 2019). In July, it is approximately 4800 m^3/s, and in August it is approximately
269 5400 m^3/s. Visual analysis of graphs given in other publications show that July flows from

glaciers are in the range of 4000 to 4800 m^3/s, and for August, the range is from 4000 to 6100 m^3/s. Lutz et al. (2014) reported the annual glacier contribution in the UIB at Bisham Qila to be 67%, which is similar to that of our simulations (Table 3).

Subbasin River Simulations

To explain the climatic and runoff conditions at the regional level, three subbasins across the UIB, namely, Gilgit, Shigar, and Kharmong were selected. These subbasins cover the entire geographic range and differ in terms of glacier coverage and climate. In total, runoff from these three subbasins contributes 35% of river flow at the Bisham Qila station, and consists of 34% glacier melt (Table 3). A common characteristic of runoff in the three subbasins at the Bisham Qila is the higher proportion of melt-runoff compared to rainfall runoff, which explains the significance of winter precipitation in the basin. Figure S6, S7, and S8 show simulations of discharge for Gilgit, Shigar, and Kharmong, respectively. They are highly glacierized, and the runoff is meltwater dependent.

Gilgit is located at the western edge of the UIB and has an elevation of 1472–6392 m. Glacier coverage in the basin is 1684 km^2 (13.2%) with almost 1181 km^2 (70%) of the glaciers located in the elevation band of 4000–5000 m. The total glacier share is 63% of the annual river flow followed by rainfall with a share of 13%.

288 The Shigar river basin lies in the northern region and has an area of 6900 km^2. This subbasin
289 has the largest glacier coverage among the subbasins of 28.8%, which contributes up to 85% of
290 the annual river flow. It is the coldest subbasin with an average annual temperature below
291 freezing. This cold climate causes most of the precipitation to fall as snow.
292 In Kharmong, rainfall runoff is more than that from glacier and snowmelt because of smaller
293 glacier cover. Glacier melt has the second highest contribution of runoff (35%), followed by
294 snowmelt (26%).
295

296 **Future Climate in the UIB**

297 Figure S9 shows the change in basin temperature and precipitation during 2075–2099 based on
298 the four MRI-AGCM scenarios. Across the UIB, the temperature will increase by 5.3 °C, and
299 the largest increase of 7–8 °C is projected to occur in the September–October period. Between
300 February–March, temperature will increase in the range of 4 °C. Precipitation will increase by
301 17% annually and, importantly, an approximately 60% increase in July–August is predicted for
302 the future precipitation regime. This trend is different from other studies for example Lutz et
303 al. (2016) used CMIP5 GCMs and reported a 25% increase in the June–September period.
304 Furthermore, Lutz et al. (2016) showed that precipitation in the future (2071–2100) will
305 decrease in the February–May season, while the GCM in this study predicts a 20% increase in

306 precipitation in 2075–2099. Another study by Su et al. (2016) employs 20 GCMs from the
307 CMIP5 annual report to project the precipitation regime over the UIB between 2041–2070.
308 However, in this study, during September–April, precipitation is simulated to either decrease
309 or remain within a change of 5% of the current precipitation. Both Su et al. (2016) and Lutz et
310 al. (2016) used similar GCMs and projected identical precipitation regimes; however, the latter
311 projects higher precipitation from September–December. This difference in future climate
312 projections is probably because Su et al. (2016) projected for 2041–2070 and Lutz et al. (2016)
313 for the subsequent 30 years (2071–2100).

314 Spatial trends in future temperature are comparatively uniform and increases across all
315 scenarios are projected (Figure 8). The warming from July to September will be the highest (7–
316 9 °C) and will result in higher quantities of glacier melt and ice loss.
317 Notably, winter temperatures (October–March) will increase by 5–6 °C, which will change the
318 form of precipitation from snowfall to rainfall. This factor has also been highlighted by Lutz et
319 al. (2016) and they projected that this phase change in precipitation will result in an increase in
320 rainfall runoff in these months.
321 On the other hand, the precipitation changes according to the MRI-AGCM scenarios are
322 spatiotemporally variable. In winter (October–March), precipitation will increase at different
323 magnitudes throughout the UIB. The eastern region of UIB is projected to have the highest

increase of up to 100% in some areas. However, spatial variations are projected during April–September (Figure 9). Summer (July–September) will have a mixed trend across the UIB. The eastern region, which comprises of the Kharmong subbasin, will record higher precipitation during July–August (Figure 9). On the contrary, the northern region where the Shigar subbasin is located will show a decrease in precipitation during the same season.

Figure 10 shows the projected monthly changes in climate in the UIB and its three subbasins. There is a consensus among the scenarios in terms of temperature change in the three subbasins. However, an insightful variability exists in the precipitation regime; Shigar will have an increase in precipitation during October–April in the future, and in Gilgit during July–September. Kharmong lies adjacent to the Himalayan mountain range, and has a different precipitation regime, which is summer dominated as opposed to that of Shigar and Gilgit. The precipitation during July–August is projected to increase by 60–80% in the subbasin.

In the UIB, precipitation will increase throughout the year; however, during March–April and July–August it will be significantly higher. This increase in precipitation will compensate for the loss of runoff because of glacier retreat in the UIB.

Future Flow Regime

Climate change will impact the peaks and quantities of the runoff components in the Bisham

342 Qila and subbasins. Figure 11 shows the seasonal alterations and shifts in the runoff components.
343 Rainfall will increase across the basin, albeit with some differences in seasonal peaks. In the
344 UIB, the spring and summer peak flows occur because of higher precipitation. These seasonal
345 trends are evident in the subbasins as well, but they have different magnitudes based on
346 variations in precipitation. There is a decrease in snowfall in the UIB and subbasins because of
347 the temperature increase, resulting in its relatively lower proportion in precipitation. Overall, at
348 the Bisham Qila station, the snowmelt runoff hydrograph will be reduced to half of its present
349 value. Furthermore, the shape of the snowmelt runoff hydrograph is likely to reduce to three
350 months, from mid-February to the end of April, in the future, while presently it lasts until June.
351 Lutz et al. (2016) also reported a decrease in the contribution of snowmelt runoff in the future
352 because rainfall will increase. Glacier retreat will cause various changes in hydrographs across
353 the UIB because of changes in climate and topographic features. In Gilgit, the glaciers will
354 retreat to the extent that it will diminish their contribution to the hydrograph. Shigar will also
355 experience a decrease in summer flows because of the retreat. On the other hand, Kharmong
356 will have an excess contribution of glaciers to the hydrograph because its glaciers are located
357 at higher elevations compared to the other two subbasins (Figure S1 b) and (Table 3).
358 Figure 12 shows the future (2075–2099) and present (1980–2005) monthly river flows at the
359 Bisham Qila station and its subbasins. At the Bisham Qila station, the annual river flow in the

360 future (2075–2099) will be 16% lower than that in 1980–2005. This decrease in the overall
361 quantities is mainly due to the lower contributions from glaciers. Even intense precipitation
362 during July–August across the UIB will not be enough to sustain the present river flows. The
363 monthly river flows will decrease during May–August because of a reduction in the
364 contribution of glaciers and lower precipitation during the May–June period. In winter and
365 spring, river flows will increase because of increase in baseflow and seasonal precipitation.
366 Other studies have also projected changes in future river flows in the UIB. For example, Lutz
367 et al. (2016) stated that under RCP 4.5 and RCP 8.5 in the future (2071–2100), river flows in
368 all seasons at the Bisham Qila station will increase, but winter flows will be substantially higher
369 because of increase in rainfall during winter and an increase in corresponding base flow.
370 Similarly, Hassan et al. (2019) reported an increase in summer river flows with a nominal
371 increase in magnitude of 1–3% and relatively higher winter river flows.
372 Gilgit and Shigar will be the most affected subbasins in the UIB. Gilgit will experience a
373 decrease every month except for March–April. Gilgit's river flows will decrease in the July–
374 September period by 85%. Likewise, Shigar's river flows are also projected to decrease by
375 approximately 45%; however, this is limited to the May–September period. Glacier retreat will
376 cause decreases in the future river flows of these two subbasins (Table 3). Soncini et al. (2015)
377 reported that, in the last decade of this century, the flows in the Shigar river basin will increase

by 27% per annum because of precipitation and excess glacier melt. However, they also have reported a decrease in summer flows. The difference between our results and their study is in the future extents of glaciers that were used for simulations. The annual average river flows in Kharmong are projected to increase in the future as evidenced from the projected increase each month. From July to September, river flows will increase up to 100% because of the combined effect of summer rainfall and glacier melt.

The Figure 13 summarizes the future river flows in the UIB and its subbasins in future (2075-2099). A drier summer is projected, on the other hand, river flows will higher in winter and spring. Significant behavior in subbasins response to climate change is also projected.

Conclusions

The UIB is the major source of water for agricultural and domestic water demands in Pakistan. Its climate is cold and the precipitation regime is winter dominated. The annual precipitation is 440 mm, most of which falls in winter as snow. Temperature-index melt models were used to calculate the snow and glacier melt in the UIB. The runoff is meltwater dominated with an annual contribution of 80% by snow and glacier melt. This high share of meltwater in runoff is also true for all the subbasins analyzed in this study.

The river flows in the UIB are vulnerable to changing climate, which cause an imbalance in the

396 water supply–demand equation. For the assessment of the impact of future climate on river
397 flows, the MRI-AGCM with a spatial resolution of 0.1875° was used. MRI-AGCM has four
398 scenarios based on different sea-level temperatures in the future (2075–2099). MRI-AGCM
399 projected a precipitation regime that will have an increase of 60–80% during July–August.
400 Besides this increase, precipitation in winter will also increase, but at a lower proportion. The
401 average temperature throughout the UIB will increase by 5.4 °C from the present values in
402 2075–2099, and the highest temperature increase of 7–8 °C is projected to take place in
403 September.
404 This increase in precipitation and temperature will alter the timings and quantities of the peak
405 flows in the UIB and its subbasins. An increase in temperature will cause the glacier and snow,
406 which are the major runoff sources, to melt early. More precipitation will occur as rainfall, and
407 thus, the contribution of snowfall to the total precipitation will decrease across the UIB. In the
408 future (2075–2099), the contribution of snow towards river flow will reduce to half of its current
409 quantities in the UIB and its subbasins. Rainfall will increase because of intense monsoons
410 across the UIB, and this increase will be pronounced during March–April. The contribution of
411 the glaciers in the subbasins towards river flows will decrease except in Kharmong, where
412 glaciers will retain most of their mass because of their higher elevation. In Gilgit, the
413 contribution of glaciers will become almost negligible compared to their present contribution.

Shigar will also record a reduction in glacier contribution, but it will not be as severe as that in Gilgit. Overall, in the UIB, glacier contribution to river flows will decrease by 25% compared to that in the present. Inclusion of the glacier mass-balance model in the present study will reveal in-depth trends in the variations of glacier hydrographs of the UIB and its subbasins.

Although the simulations of river flows in the UIB and subbasins were satisfactory and match well with those of other studies, several improvements are recommended. The precipitation datasets should be corrected using multiple precipitation extrapolation rates owing to the variability of climate in the basin. Moreover, improvements in melt models are crucial for accurate estimation of snowfall, glacier/snow melt, and runoff. Glacier mass-balance models need to be included in future simulations of areas where glacier retreat plays a crucial role in annual river flows.

Inclusion of the fine-resolution GCM has revealed an important pattern of future climate in the UIB in the form of intense summer rainfall. This rainfall plays a crucial role in the dry season. The modelled alterations in the peaks of the runoff components will result in a reduction in the average annual river flow in the UIB. Seasonal changes are very important because they provide flow for irrigation, hydro-power generation, and storage from September to April, while there is an imbalance in the demand–supply equation in the remaining months. The downstream regions will have to share this imbalance and adapt to the changes in timing and quantities.

Abbreviations

APHRODITE: Asian precipitation highly resolved observational data integration towards evaluation; GCM: General circulation model; ICIMOD: International Centre for Integrated Mountain Development; MODIS: Moderate Resolution Imaging Spectroradiometer; MRI-AGCM: Meteorological Research Institute atmospheric general circulation model; RCM: Regional Climate Model; RCP: Representative Concentrative Pathway; RRI: Rainfall–runoff–inundation; UIB: Upper Indus River Basin

Declarations

Availability of data and material

The additional information is available in the Supplementary file.

Competing interests

The authors declare that they have no competing interest.

Authors' contributions

SB and TS conceptualized the study. SB prepared the dataset and performed the modeling tasks. MY contributed in glacier melt analysis. SB wrote the manuscript and all the authors

contributed in the and review.

Acknowledgements

Funding: SB is funded by Japanese government through the MEXT scholarship for PhD studies at Kyoto university. In addition to this, the authors are thankful to Kyoto University for providing additional funding for data collection.

Special thanks to the Water and Power Development Authority (WAPDA) and Pakistan Meteorological Authority (PMD) for the provision of hydro-meteorological data.

References

Ali A (2013) Indus Basin floods: Mechanisms, Impacts, and Management. Asian Development Bank. Available via: https://hdl.handle.net/11540/810. Accessed 12 January 2021

Archer D (2003) Contrasting hydrological regimes in the upper Indus Basin. J. Hydrol 274(1–4):198–210

Dahri ZH, Moors E, Ludwig F, Ahmad S, Khan A, Ali I, Kabat P (2018) Adjustment of measurement errors to reconcile precipitation distribution in the high-altitude Indus basin. Int. J. Climatol 38:3842-3860. doi: 10.1002/joc.5539

Hassan M, Du P, Mahmood R, Jia S, Iqbal W (2019) Streamflow response to projected climate

468 changes in the Northwestern Upper Indus Basin based on regional climate model (RegCM4.3)
469 simulation. J. Hydro-Environment Res. 27:32-49. doi.org/10.1016/j.jher.2019.08.002
470 Hasson S ul, Saeed F, Böhner J, Schleussner CF (2019) Water availability in Pakistan from
471 Hindukush–Karakoram–Himalayan watersheds at 1.5 °C and 2 °C Paris Agreement targets. Adv.
472 Water Resour. 131: Art. 103365. doi.org/10.1016/j.advwatres.2019.06.010
473 Huss M, Hock R (2015) A new model for global glacier change and sea-level rise. Front. Earth
474 Sci 3:54. doi: 10.3389/feart.2015.00054
475 ICIMOD. Clean Ice and Debris covered glaciers of HKH Region (2011) Available via:
476 http://apps.geoportal.icimod.org/hkhglacier. Assessed 30 August 2020
477 Immerzeel WW, van Beek LPH, Bierkens MFP (2010) Climate change will affect the Asian
478 water towers. Science 328(5984):1382–1385. doi:10.1126/science.1183188
479 Immerzeel WW, Wanders N, Lutz AF, Shea JM, Bierkens MFP (2015) Reconciling high-
480 altitude precipitation in the upper Indus basin with glacier mass balances and runoff. Hydrol.
481 Earth Syst. Sci 19:4673–87. doi: 10.5194/hess-19-4673-2015
482 Lutz AF, Immerzeel WW, Kraaijenbrink PDA, Shrestha AB, Bierkens MFP (2016) Climate
483 change impacts on the upper indus hydrology: Sources, shifts and extremes. PLoS One.
484 doi.org/10.1371/journal.pone.0165630
485 Lutz AF, Immerzeel WW, Shrestha AB, Bierkens MFP (2014) Consistent increase in High

Asia's runoff due to increasing glacier melt and precipitation. Nat. Clim. Chang 4:587–91. doi: 10.1038/nclimate2237

Mcsweeney C, New M, Lizcano G (2012) UNDP Climate Change Country Profiles Pakistan. Available via: http://country-profiles.geog.ox.ac.uk.Assessed 19 November 2020

Miao C, Su L, Sun Q, Duan Q (2016) A nonstationary bias-correction technique to remove bias in GCM simulations. J. Geophys. Res 121:5718-5735. doi.org/10.1002/2015JD024159

Mizuta R, Yoshimura H, Murakami H, Matsueda M, Endo H, Ose T, Kamiguchi K, Hosaka M, Sugi M, Yukimoto S, Kusunoki S, Kitoh A (2012) Climate Simulations Using MRI-AGCM3.2 with 20-km Grid. J. Meteorol. Soc. Japan 90A(0):233–58. doi:10.2151/jmsj.2012-A12

Mukhopadhyay B, Khan A (2014) A quantitative assessment of the genetic sources of the hydrologic flow regimes in Upper Indus Basin and its significance in a changing climate. J. Hydrol 509:549-572. doi: 10.1016/j.jhydrol.2013.11.059

Mukhopadhyay B, Khan A (2015) A reevaluation of the snowmelt and glacial melt in river flows within Upper Indus Basin and its significance in a changing climate. J. Hydrol 527:119–32. doi: 10.1016/j.jhydrol.2015.04.045

Reggiani P, Rientjes THM (2015) A reflection on the long-term water balance of the Upper Indus Basin. Hydrol. Res 46:446-462. doi: 10.2166/nh.2014.060

Rounce DR, Hock R, Shean DE (2020) Glacier Mass Change in High Mountain Asia Through

2100 Using the Open-Source Python Glacier Evolution Model (PyGEM). Front. Earth Sci. 7:331. doi: 10.3389/feart.2019.00331

Sanjay J, Krishnan R, Shrestha AB, Rajbhandari R, Ren GY (2017) Downscaled climate change projections for the Hindu Kush Himalayan region using CORDEX South Asia regional climate models. Adv. Clim. Chang. Res. 8:185-198. doi: 10.1016/j.accre.2017.08.003

Sayama T (2015) RRI User manual. Available via: http://www.icharm.pwri.go.jp/research/rri/rri_top.html. Assessed 15 September 2020

Sayama T, Ozawa G, Kawakami T, Nabesaka S, Fukami K (2012) Rainfall–runoff–inundation analysis of the 2010 Pakistan flood in the Kabul River basin. Hydrol. Sci. J. 57:298-312. doi: 10.1080/02626667.2011.644245

Soncini A, Bocchiola D, Confortola G, Bianchi A, Rosso R, Mayer C, Lambrecht A, Palazzi E, Smiraglia C, Diolaiuti G (2015) Future hydrological regimes in the upper Indus basin: A case study from a high-altitude glacierized catchment. J. Hydrometeorol 16:306-326. doi: 10.1175/JHM-D-14-0043.1

Su F, Zhang L, Ou T, Chen D, Yao T, Tong K, Qi Y (2015) Hydrological response to future climate changes for the major upstream river basins in the Tibetan Plateau. Glob. Planet. Change 136:82-95. doi: 10.1016/j.gloplacha.2015.10.012

Terink W, Lutz AF, Simons GWH, Immerzeel WW, Droogers P (2015) SPHY v2.0: Spatial

Processes in HYdrology. Geosci. Model Dev 8:2009-2034. doi: 10.5194/gmd-8-2009-2015

Valéry A, Andréassian V, Perrin C (2014) "As simple as possible but not simpler": What is useful in a temperature-based snow-accounting routine? Part 2 - Sensitivity analysis of the Cemaneige snow accounting routine on 380 catchments. J. Hydrol 517-1176-1187. doi: 10.1016/j.jhydrol.2014.04.058

Wester P, Mishra A, Mukherji A, Shrestha AB (2019) The Hindu Kush Himalaya Assessment: Mountains, Climate Change, Sustainability and People. Available via: https://link.springer.com/book/10.1007%2F978-3-319-92288-1. Assessed 19 October 2020

Yatagai A, Kamiguchi K, Arakawa O, Hamada A, Yasutomi N, Kitoh A (2012) Aphrodite constructing a long-term daily gridded precipitation dataset for Asia based on a dense network of rain gauges. Bull. Am. Meteorol. Soc 93:1401-1415. doi: 10.1175/BAMS-D-11-00122.1

Figure legends

Figure 1. Map of the upper Indus river basin with its outlet at Bisham Qila.

Figure 2. Upper Indus river basin and its subbasins with their elevations.

Figure 3. Spatial distribution of average temperature and precipitation in the UIB (1980–2005).

Figure 4. Flow chart explaining the data and models used in this study.

Figure 5. Calibration and validation results of the hydrological model at Bisham Qila.

Figure 6. Comparison of MODIS snow cover with simulated snow cover.

Figure 7. Monthly contribution of glacier, snow, and rain in the UIB (1980–2005).

Figure 8. Increase in temperature across 4 MRI-AGCM scenarios based on seasons.

Figure 9. Change in precipitation across 4 MRI-AGCM scenarios on based on seasons.

Figure 10. Change in climate in the subbasins of the UIB according to four MRI-AGCM scenarios (left: monthly temperature; right: monthly precipitation).

Figure 11. Comparison between present and future runoff components of the UIB and subbasins. Row wise the simulations represent Bisham Qila, Gilgit, Shigar and Kharmong respectively. Black line represents present and other colors MRI-AGCM simulations.

Figure 12. Present and future river flows in the UIB and subbasins. Present river flows are shown in black.

558 Figure 13. Percentage changes in the monthly river flows in future (2075-2099) in UIB and its

559 subbasins with respect to present (1980-2005).

Figures

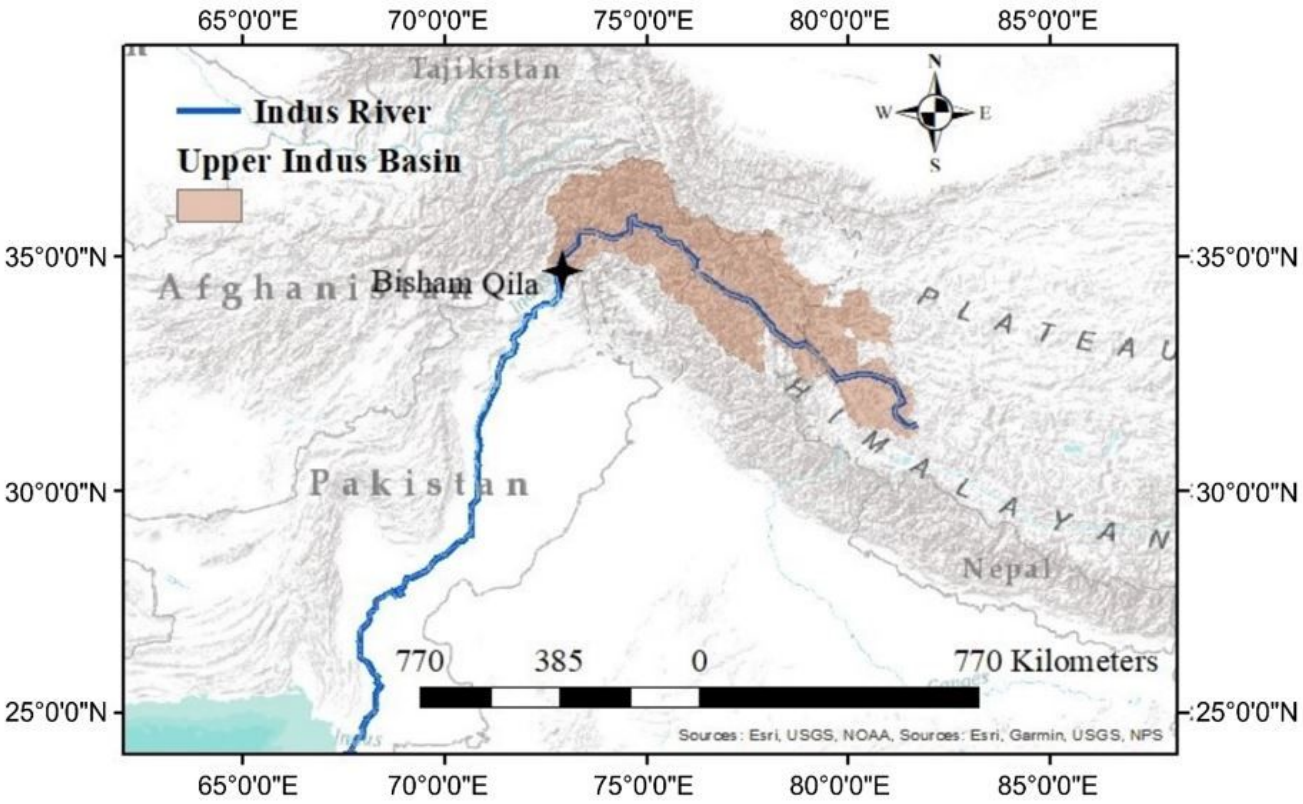

Figure 1

Map of the upper Indus river basin with its outlet at Bisham Qila. Note: The designations employed and the presentation of the material on this map do not imply the expression of any opinion whatsoever on the part of Research Square concerning the legal status of any country, territory, city or area or of its authorities, or concerning the delimitation of its frontiers or boundaries. This map has been provided by the authors.

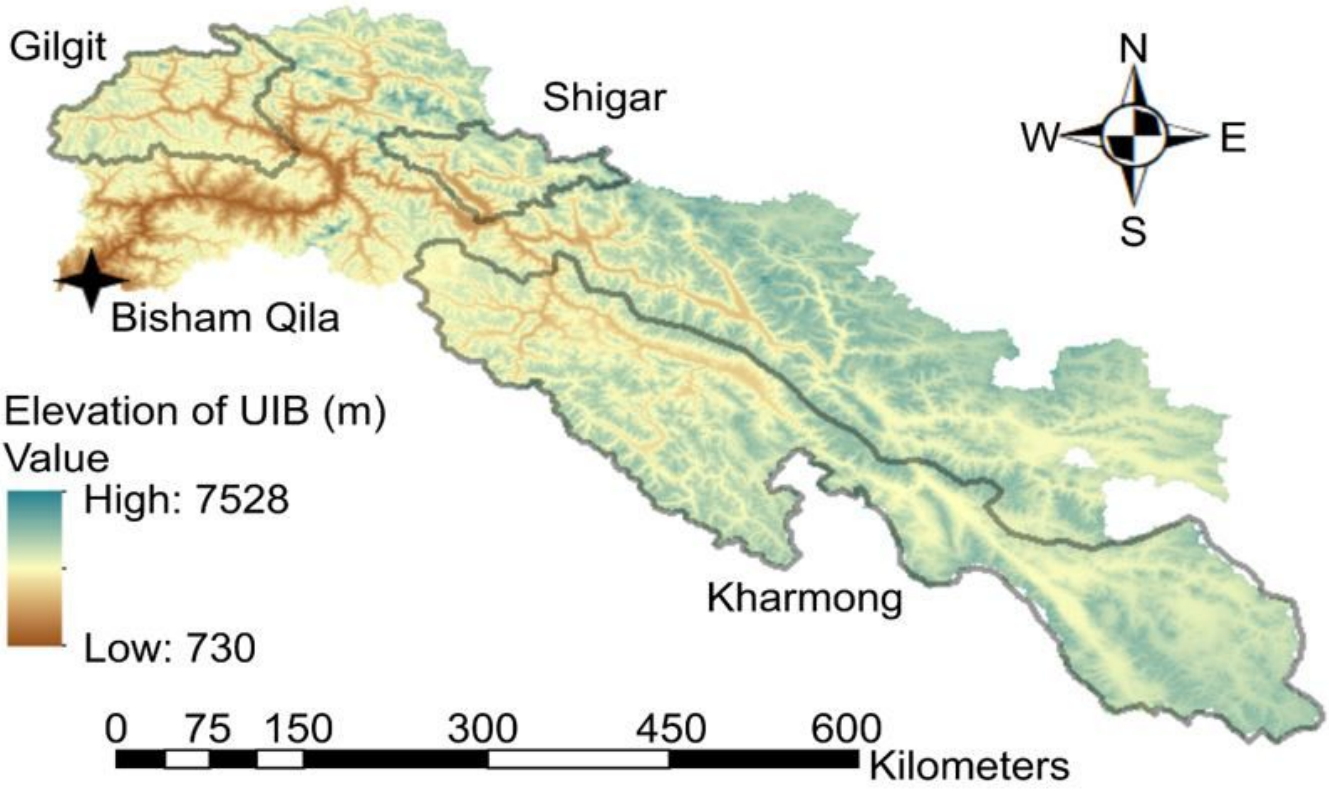

Figure 2

Upper Indus river basin and its subbasins with their elevations. Note: The designations employed and the presentation of the material on this map do not imply the expression of any opinion whatsoever on the part of Research Square concerning the legal status of any country, territory, city or area or of its authorities, or concerning the delimitation of its frontiers or boundaries. This map has been provided by the authors.

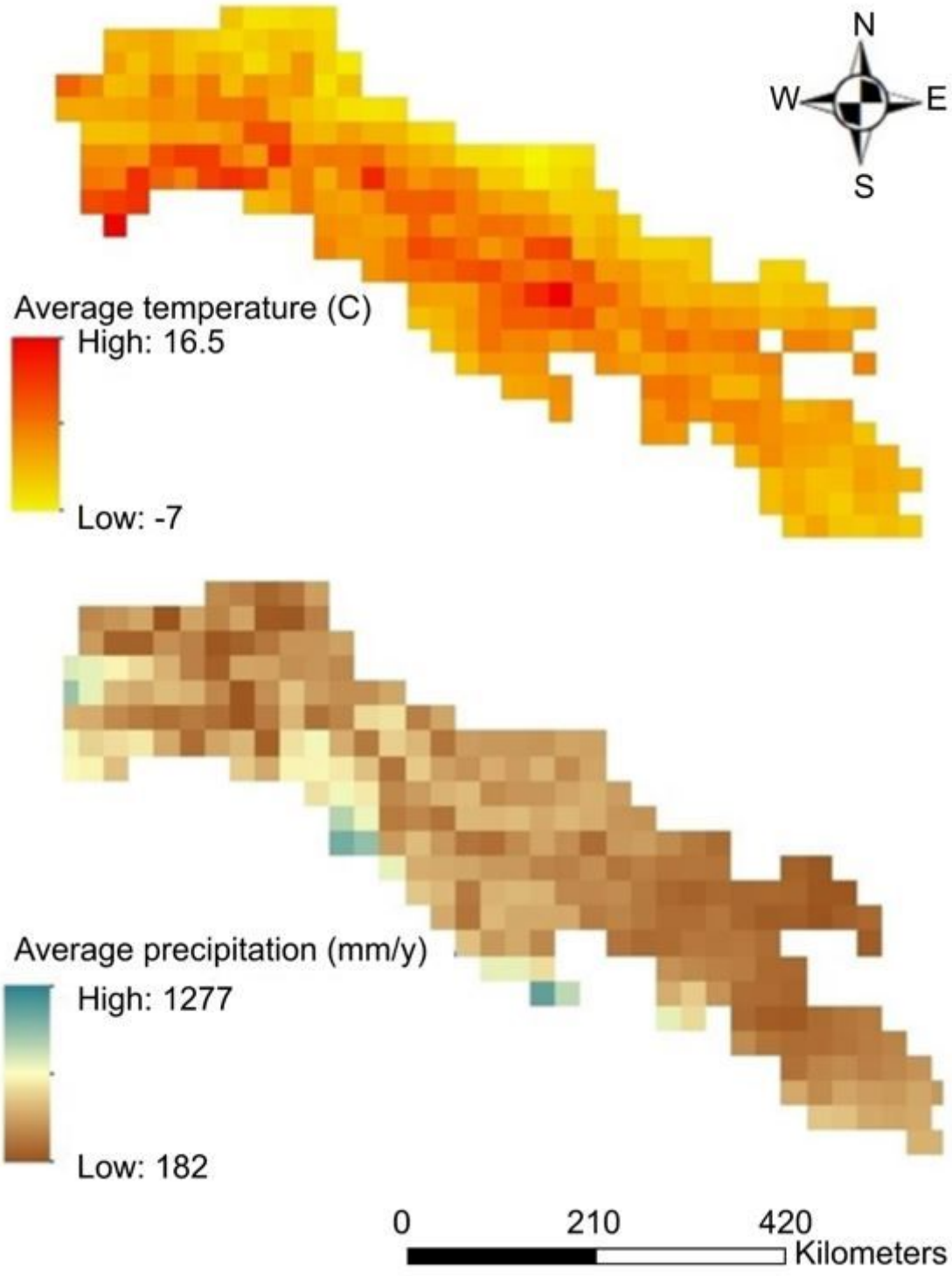

Figure 3

Spatial distribution of average temperature and precipitation in the UIB (1980–2005). Note: The designations employed and the presentation of the material on this map do not imply the expression of any opinion whatsoever on the part of Research Square concerning the legal status of any country, territory, city or area or of its authorities, or concerning the delimitation of its frontiers or boundaries. This map has been provided by the authors.

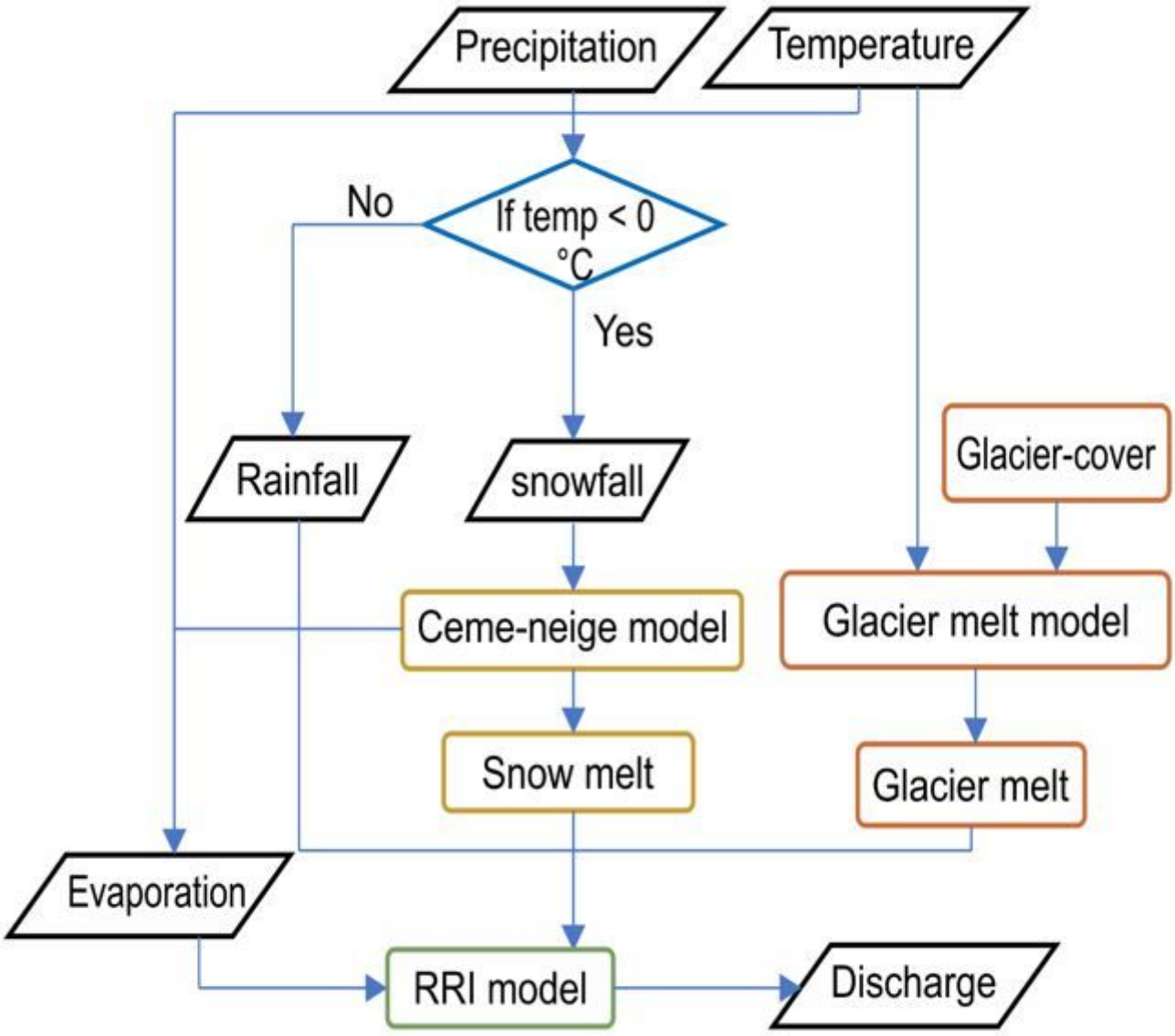

Figure 4

Flow chart explaining the data and models used in this study.

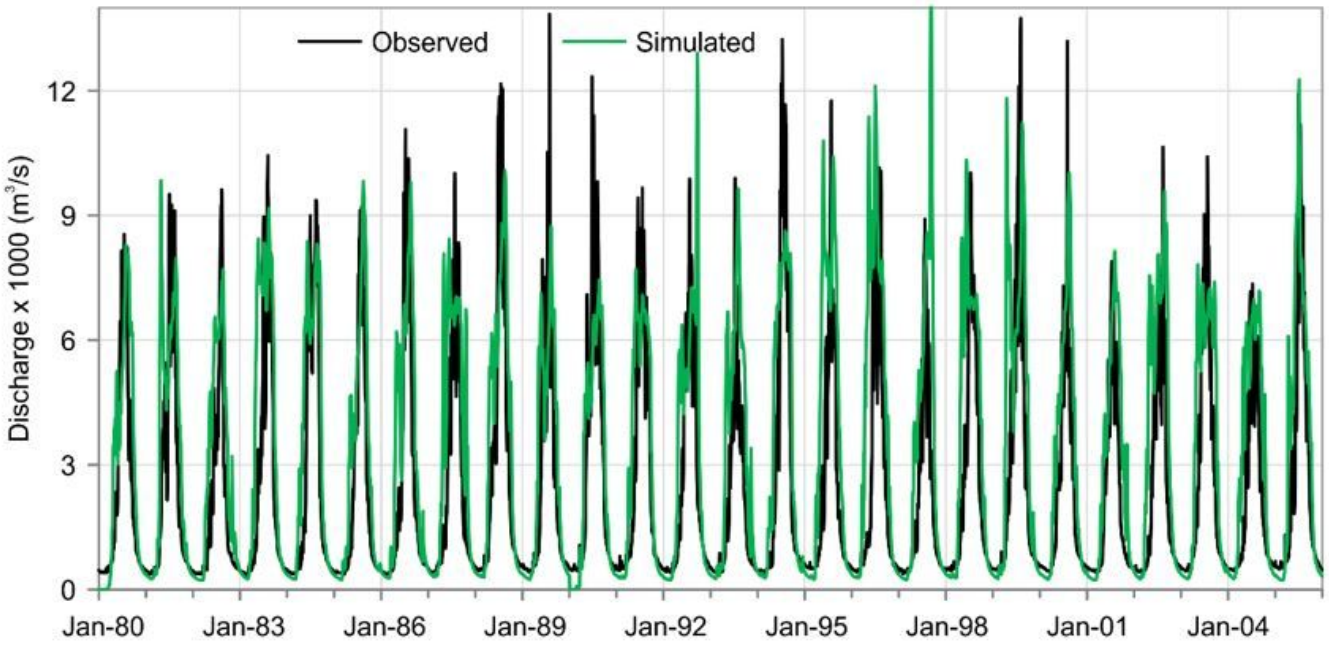

Figure 5

Calibration and validation results of the hydrological model at Bisham Qila.

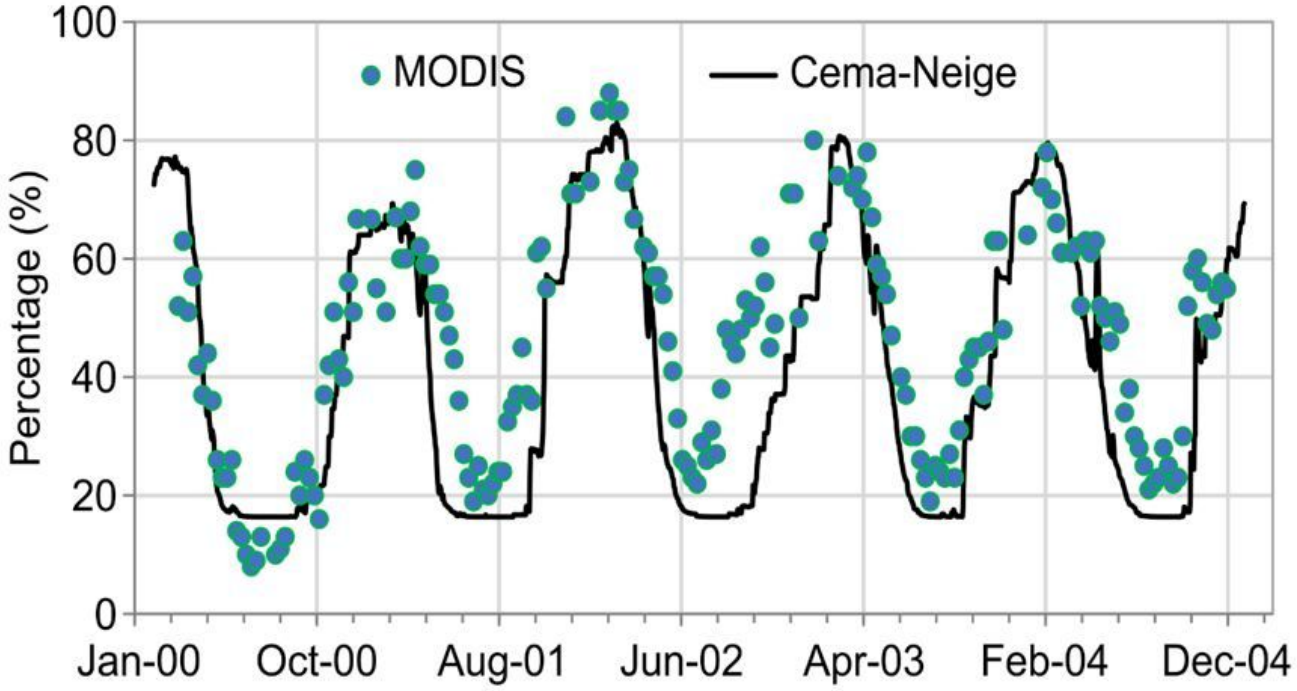

Figure 6

Comparison of MODIS snow cover with simulated snow cover.

Figure 7

Monthly contribution of glacier, snow, and rain in the UIB (1980–2005).

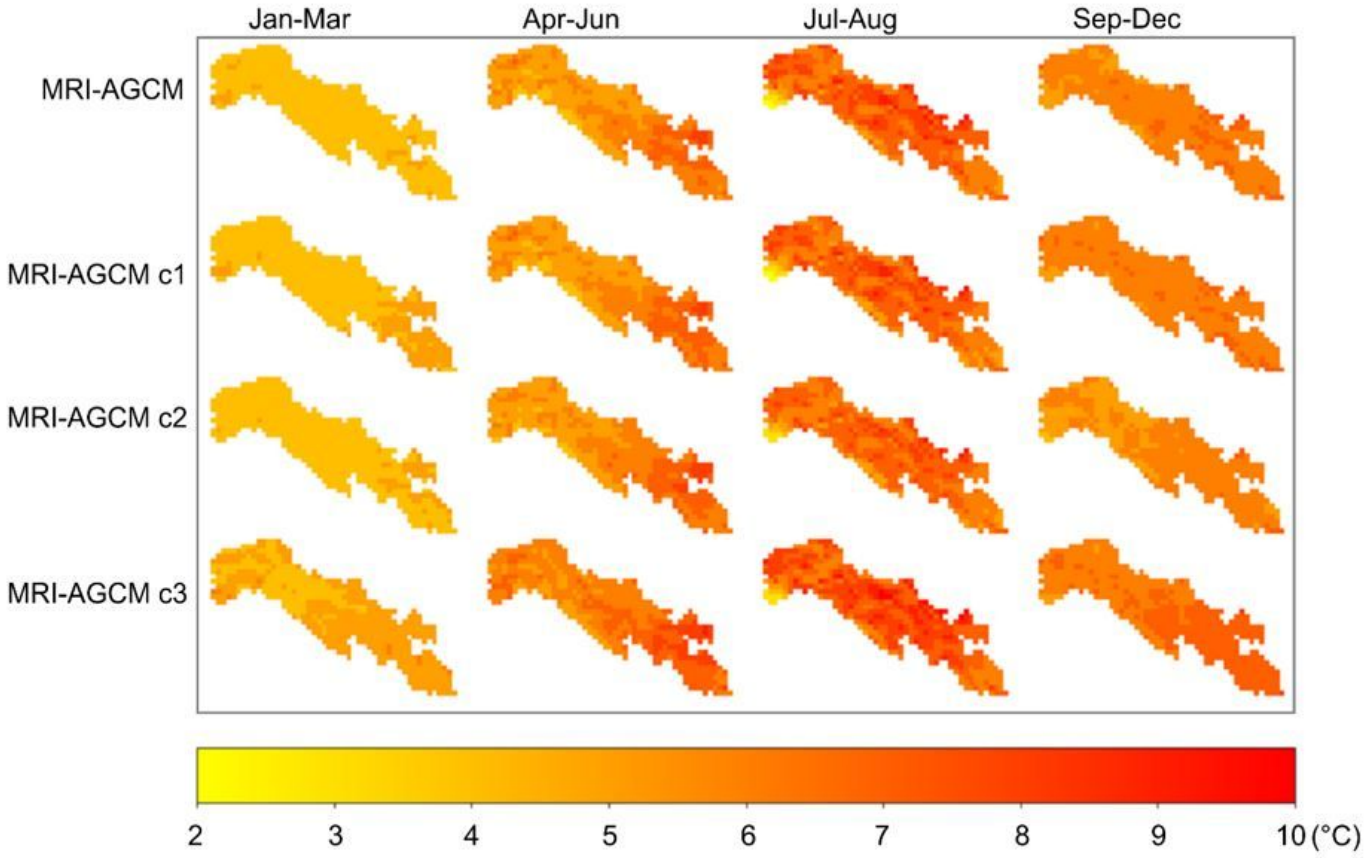

Figure 8

Increase in temperature across 4 MRI-AGCM scenarios based on seasons. Note: The designations employed and the presentation of the material on this map do not imply the expression of any opinion whatsoever on the part of Research Square concerning the legal status of any country, territory, city or area or of its authorities, or concerning the delimitation of its frontiers or boundaries. This map has been provided by the authors.

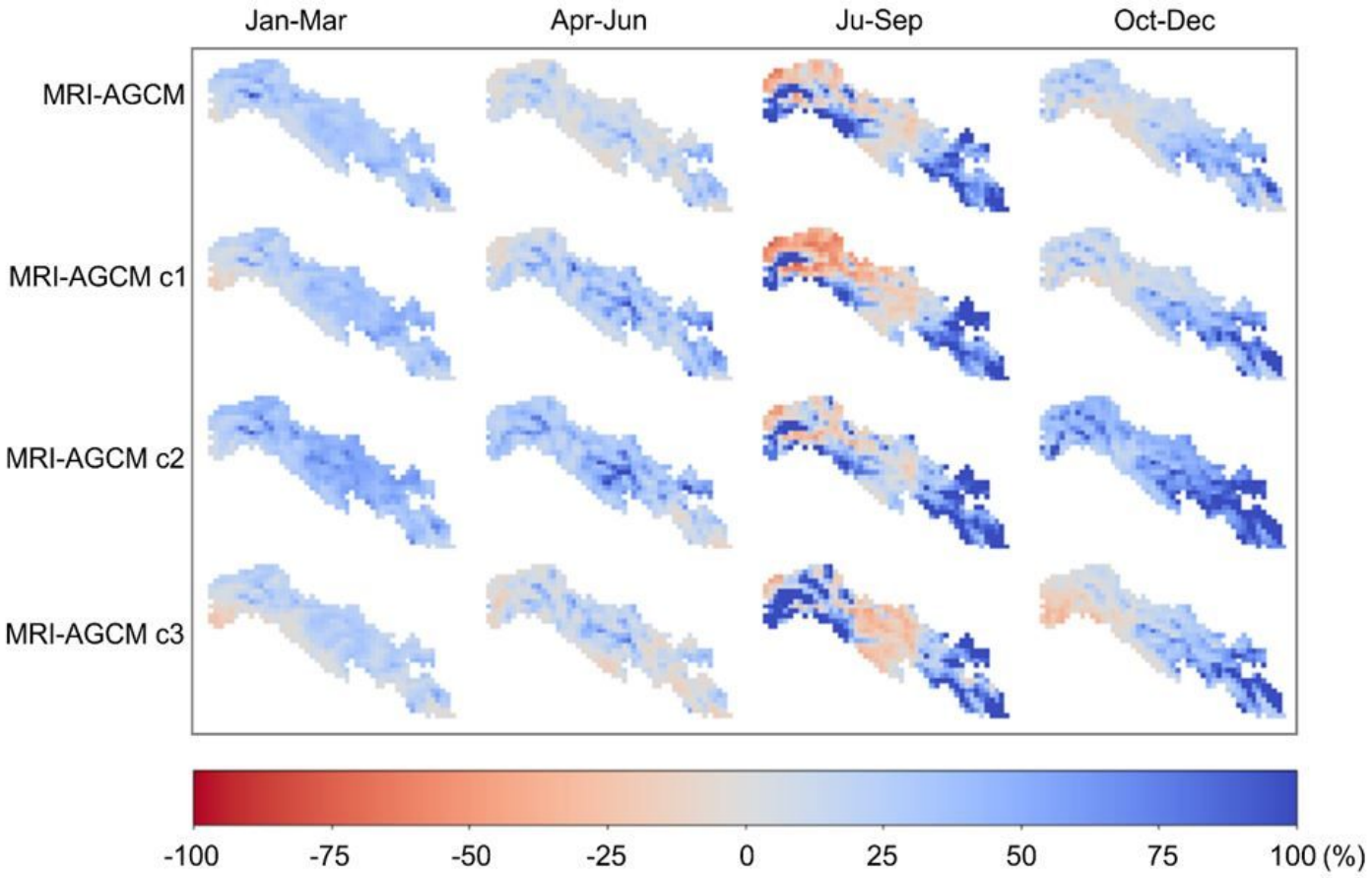

Figure 9

Change in precipitation across 4 MRI-AGCM scenarios on based on seasons. Note: The designations employed and the presentation of the material on this map do not imply the expression of any opinion whatsoever on the part of Research Square concerning the legal status of any country, territory, city or area or of its authorities, or concerning the delimitation of its frontiers or boundaries. This map has been provided by the authors.

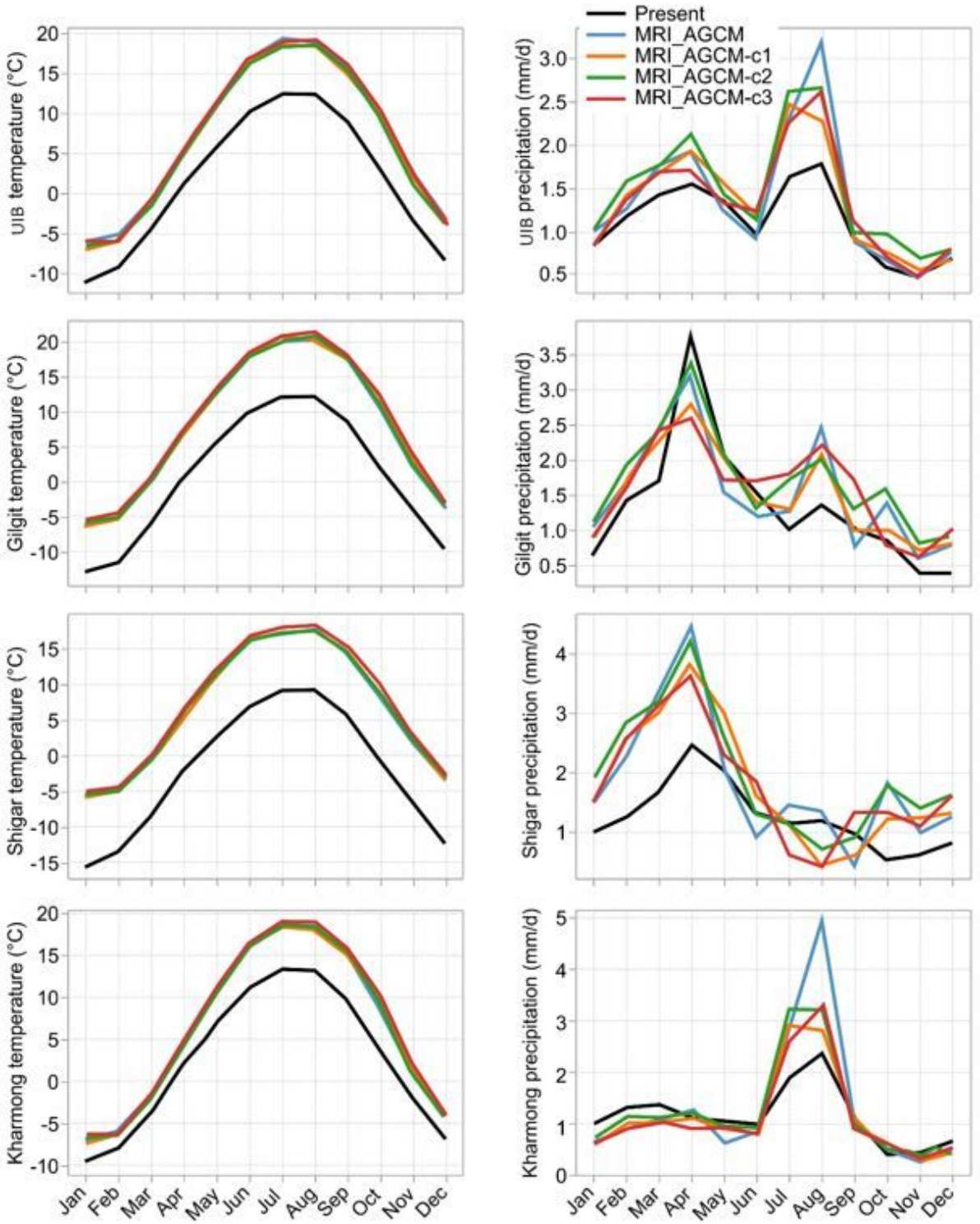

Figure 10

Change in climate in the subbasins of the UIB according to four MRI-AGCM scenarios (left: monthly temperature; right: monthly precipitation).

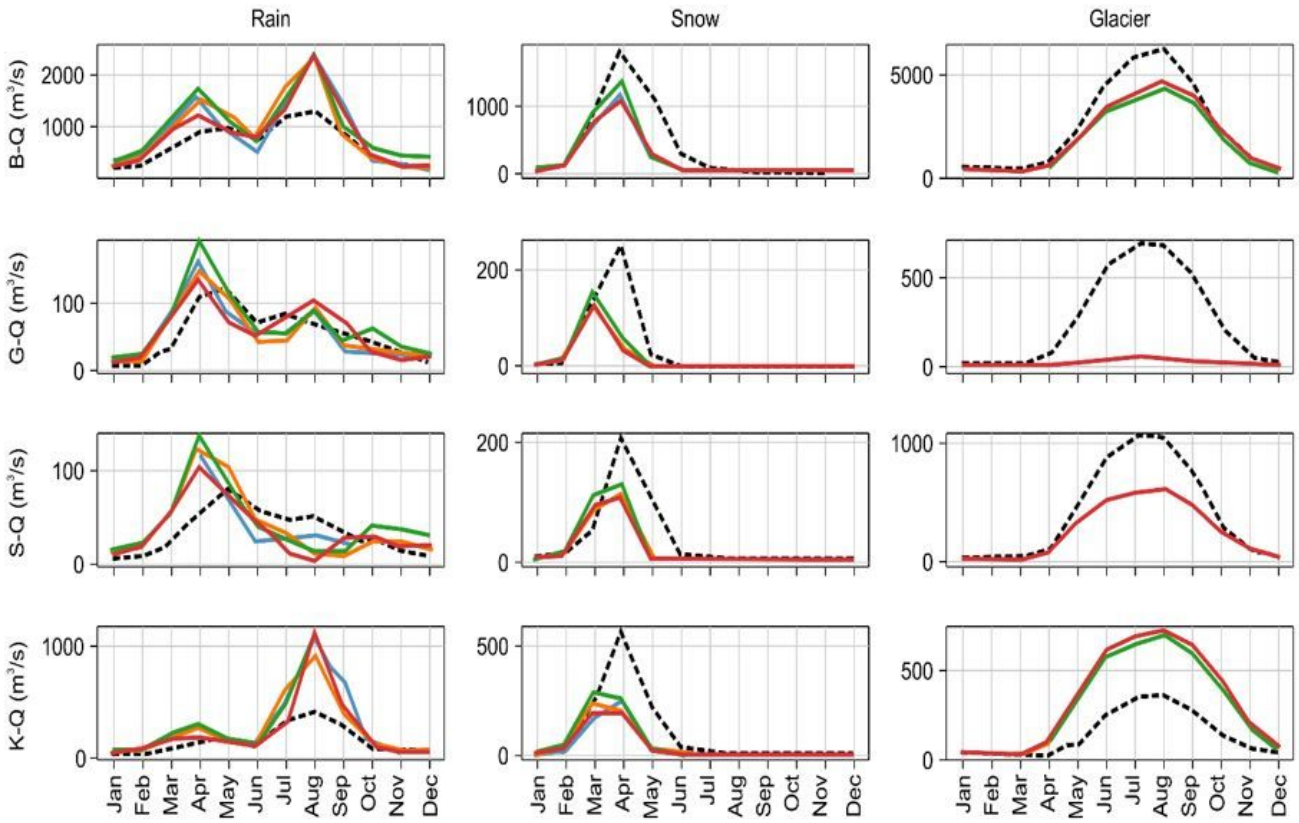

Figure 11

Comparison between present and future runoff components of the UIB and subbasins. Row wise the simulations represent Bisham Qila, Gilgit, Shigar and Kharmong respectively. Black line represents present and other colors MRI-AGCM simulations.

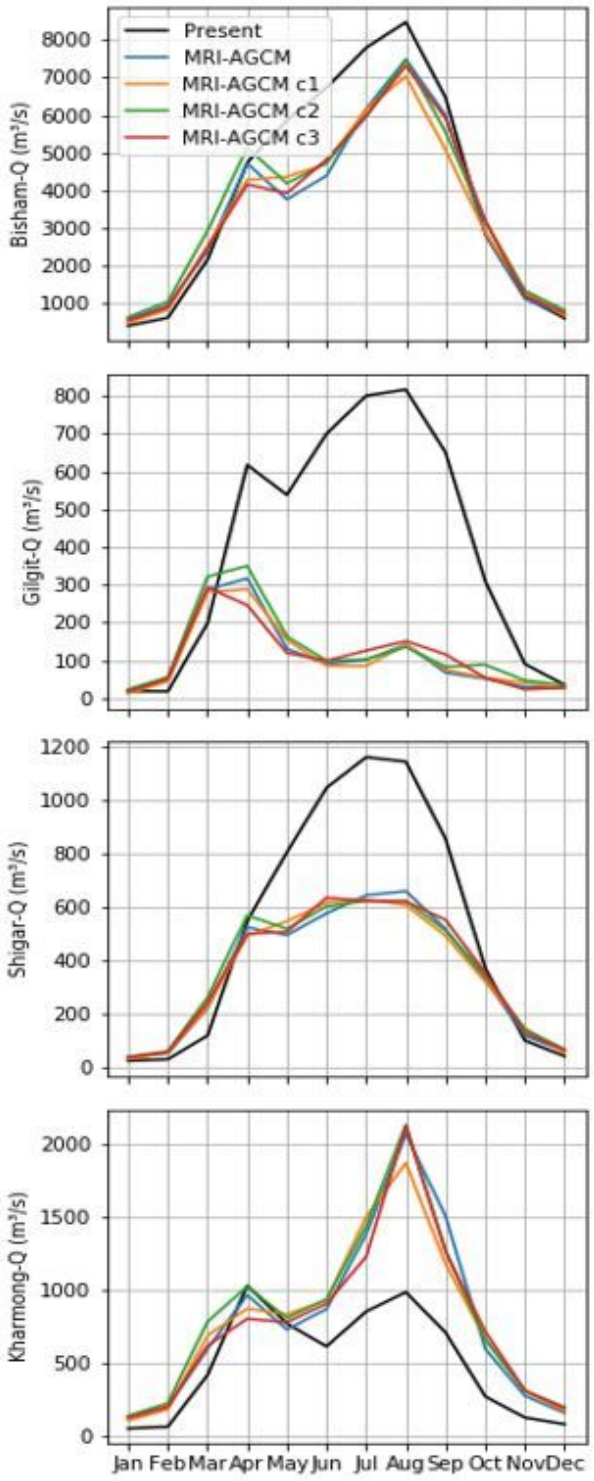

Figure 12

Present and future river flows in the UIB and subbasins. Present river flows are shown in black.

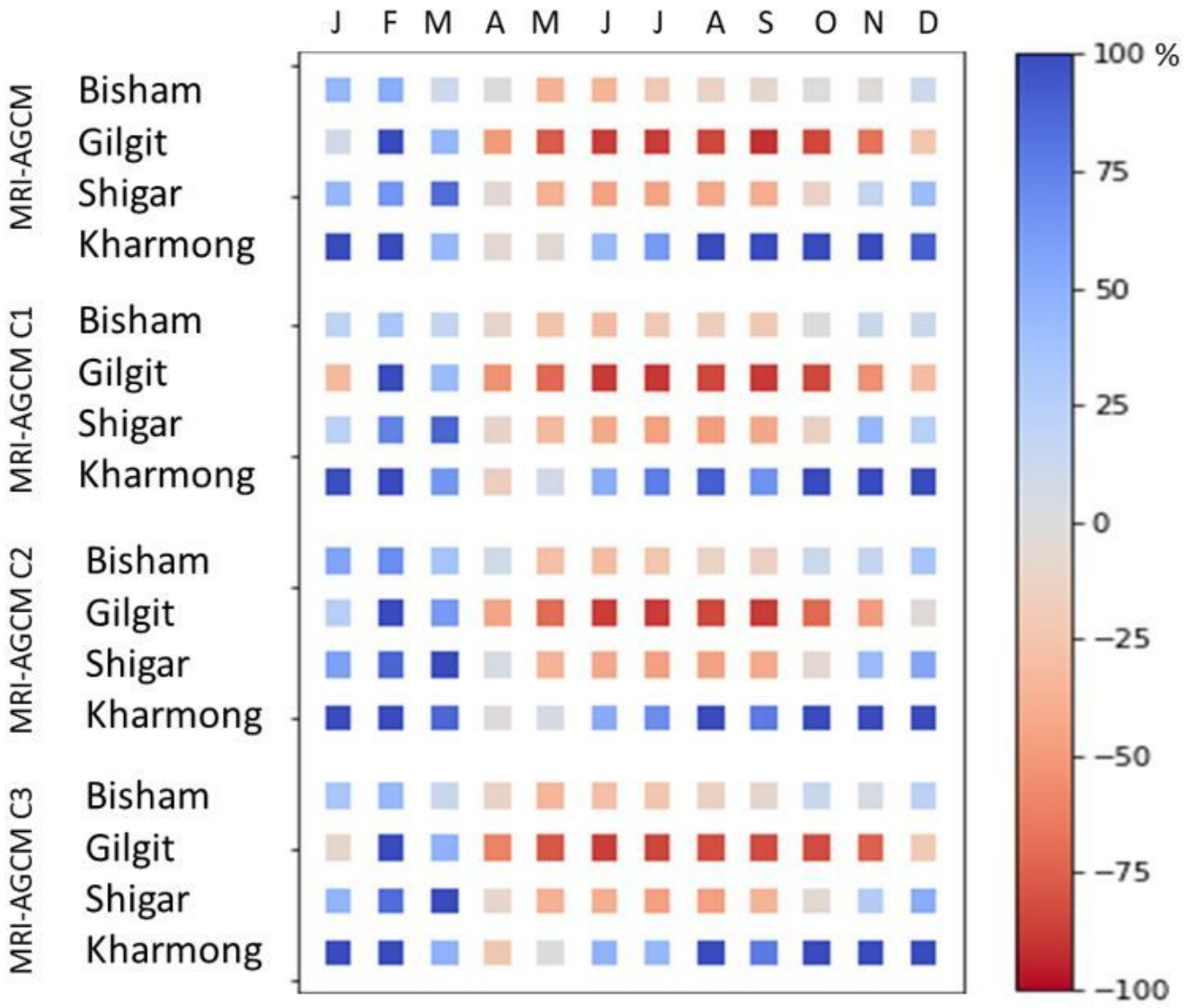

Figure 13

Percentage changes in the monthly river flows in future (2075-2099) in UIB and its subbasins with respect to present (1980-2005).

Supplementary Files

This is a list of supplementary files associated with this preprint. Click to download.

- graphicalabstract.docx
- SupplementaryMaterial.docx